JOURNAL OF CRITICAL REVIEWS

ISSN- 2394-5125VOL 7, ISSUE 15, 2020

STATISTICAL INVESTIGATION OF ACCURACY OF SATELLITE ELEVATION DATA: A CASE STUDY

SIDHARTHA SAWAI[1], KISHAN SINGH RAWAT[1*], SUDHIR KUMAR SINGH[2], SANJEEV KUMAR[1]

[1,2,4] Geo-Informatics, Civil Engineering Department, Graphic Era (Deemed to be University) Dehradun, (Uttrakhand), India

[2]K. Banerjee Centre of Atmospheric Ocean Studies, IIDS, Nehru Science Centre, University of Allahabad, Prayagraj, (Uttar Pradesh), India

[*] ksr.kishan@gmail.com

Received: 14 April 2020 Revised and Accepted: 8 August 2020

ABSTRACT:

In this work we have used SRTM 90 and 30m, ASTER 30m and 60 cm Google Earth (GE) based elevation data generated using online tool Terrain Zonum, validation was performed with respect to Survey of India (SOI) toposheet. These results are important for those areas where limited field data are available. It also provides a benchmark for validation of future DEM with respect to SOI toposheet. Statistical tests were applied to assess vertical accuracy.

The results highlight a minimum and maximum RMSE of 1.54m and 3.75m for temples and settlement, SRTM-30m, ASTER-30m and temples (1.84m) and 4.54m (for settlement) respectively with respect to SOI toposheet. Similarly, SRTM-90m indicate min and max RMSE of 1.88m and 6.57m for temples and other type of trees respectively. While Google Earth (GE) model show minimum 16.08m (for settlement) and maximum is 29.35m (for temples). We observed that SRTM-30m has good vertical accuracy for all classes (forest, towers, settlement, boundary pillars, temples and other types of tree). SRTM-30m score first rank for study area (Tehri District of Uttarakand, India) on the basis of statistical analysis.

KEYWORDS: Google earth; vertical accuracy; DEM; DSM; RMSE

I. INTRODUCTION

Digital elevation model (DEM) has variety of applications in different fields. The most used DEM data is of SRTM which has different resolution (1 and 3 arc seconds). SRTM DEM is generated through Synthetic Aperture Radar (SAR) technique. Both resolutions of SRTM DEM are open access. ASTER DEM covers 83° north latitude and 83° south from equator currently ASTER GDEM (3generation) is also freely available.

The literature outlined applications of DEM different field such as hydrology (Kumar et al. 2018a), geomorphology, morphometry (Yadav et al. 2014; Choudhari et al. 2018; Singh and Singh 2018; Yadav et al. 2018; Kumar et al. 2018a; Yadav et al. 2020), morphotectonics, forestry (Srivatava et al. 2019), urban planning (Singh et al. 2015), soil erosion (Pradhan et al. 2020; Maliqi and Singh 2019), groundwater potential zone (Singh et al. 2010; Pande et al. 2019; Murmu et al. 2019), watershed management (Kumar et al. 2017; Kumar et al. 2018b; Narsimlu et al. 2015), infrastructural facility development and geoenvironmental hazard (Stankevich et al. 2020) etc. Such types of studies are heavily relied on the accurate availability of DEM data.

Previous work performs the comparative evaluation of DEM with respect to ground observation in order to identify the vertical and horizontal accuracy of DEM (Rusli et al. 2014; Yarrakula and Samanta 2013; Suwandana et al. 2012). Rusli et al. (2014) has evaluated the vertical accuracy for flat, hilly and mountainous height points obtained from Google Earth with ASTER and SRTM. The accuracy of SRTM DEM is very much close to the contour-based DEM obtained from Survey of India toposheet (Kumar 2013). Hui and Zhao (2018) performed a study to compare accuracy of global 1 arc-second ALOS world 3D-30 m DEM using ICESat/GLAS data and reported that AW3D30 is better compared to SRTM 1 arc-second data. ASTER (V2), SRTM 3 arc-second, CARTOSAT-1 and topographical maps (R.F. 1:250,000 and 1:50,000), have been used to extract and analyse the morphotectonic properties of a mountainous drainage basin and found the ASTER (V2) has good accuracy (Das et

ISSN- 2394-5125VOL 7, ISSUE 15, 2020

al. 2016). Szabo et al. (2015) have identified that slope angle and aspect influence the SRTM and ASTER GDEM accuracy. Rawat et al. (2019a) studied the vertical accuracy SRTM, ASTER DEM and compared to CARTOSAT-1 DEM.

In DEM errors arises due many factors namely data acquisition, systematic errors, non-systematic errors and terrain specific ambiguity which are difficult to avoid (Patel et al. 2016). Hence, the following objectives of the study were conceptualized to (i) evaluate vertical accuracy of DEM of SRTM-30 & 90m, ASTER-30m and Google Earth (GE), and (ii) rank the DEM model for specific classes.

II. METHODOLOGY

2.1 Study area

Area lies in Uttarakhand state, India, Tehri Garhwal has hilly terrain and its administrative headquarter is at New Tehri. The district is surround by Rudraprayag in the east, Dehradun in the west, Uttarkashi in the north, and Pauri Garhwal in the south. Four SOI toposheet cover the district and two falls in the category of classified/restricted (Topo sheet No:$53\frac{J}{11}$ and$53\frac{J}{12}$), and hence two toposheets No:$53\frac{J}{7}$ and $53\frac{J}{8}$ were used for this work.

The minimum temperature in summer remains 9 °C and 3 °C in winters. However, the temperature in Tehri Garhwal shoots up to 30 °C in summers and 15 °C in winters. The average annual rainfall about 70 cms. In about 70 percent of the area of the district where slopes are steep to very steep, topography was revealed to be the dominant factor determining characteristic soil development. In the remaining part where slopes are moderate to gentle, parent material is the dominant factor followed by topography. Wheat, barley, masoor, red gram, mustard and pea during dry season. Whereas during wet season rice, barnyard millet, finger millet, black gram and soyabean are grown in the region.

2.2 Data used

There are four open source of elevation data were used in present study (Table 1). Like SRTM-30 and SRTM-90m are different in resolution but same in technology (SAR). SRTM-30m and ASTER-30m (based on thermal remote sensing technology) are same in resolution but different in technology. Similarly, elevation information from GE (based on aerial photography technology) also different in resolution and technology wise from other source of elevation information.

Table 1 Summary for elevation information sources

Elevation data	Summary statistics for elevation		
	Resolution	Technology	Source
SRTM	30m	SIR-C/X-SAR	http://srtm.csi.cgiar.org/download
SRTM	90m	SIR-C/X-SAR	http://srtm.csi.cgiar.org/download
ASTER	30m	Thermal	gdem.ersdac.jspacesystems.or.jp
Google Earth	0.15m (highest)	Aerial photography	Google Earth & zonums.com/gmaps/terrain.php

ISSN- 2394-5125VOL 7, ISSUE 15, 2020

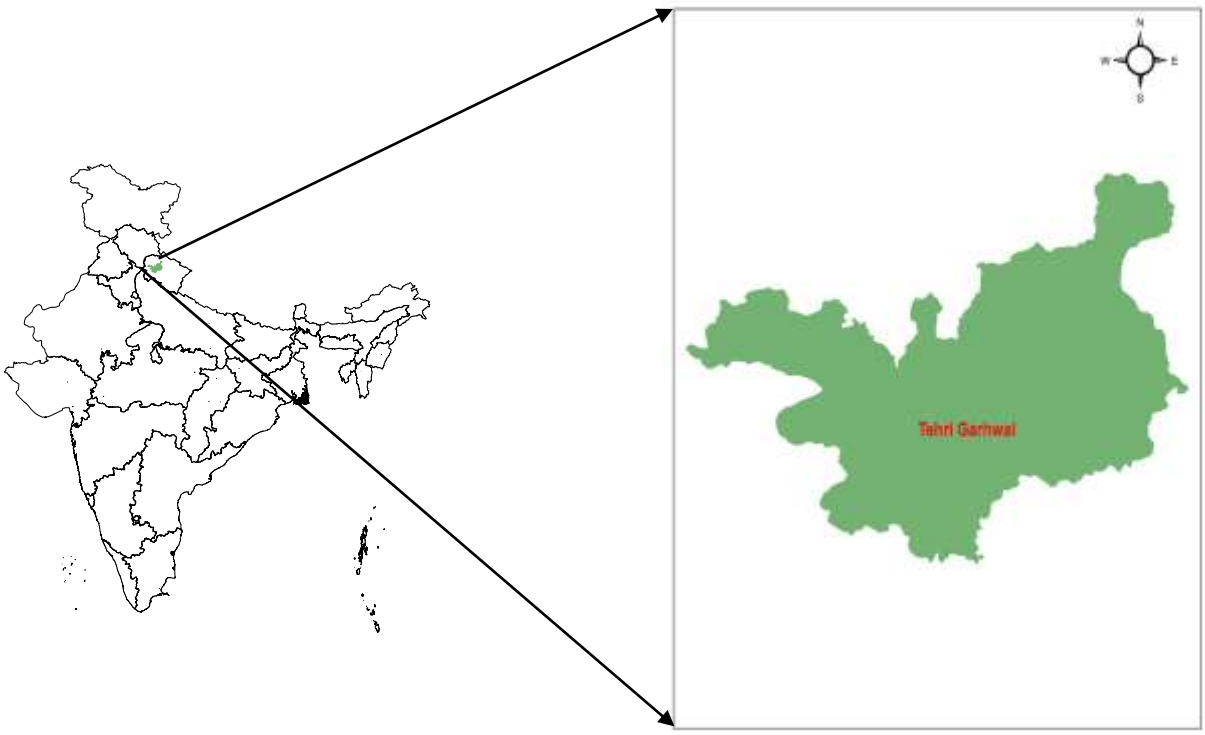

Fig.1. Map of study area

2.3 Statistical tests for performance evaluation

2.3.1 Standard Error of Estimation (SEE)

The variation of observation made of the accuracy of predictions which is made by the line that shortens the sum of squared deviations of predictions (Rawat et al. 2017). The formula of SEE is give below eqn. (1):

$$\boldsymbol{SEE_M} = \left(\frac{\sum_{i=1}^{n}(V_O - V_M)^2}{n-1}\right)^{0.5} \quad (1)$$

where, V_O represent to reference whereas V_M is model value and n is a total number of observations.

2.3.2 Root Mean Square Error (RMSE)

RMSE is used to measure of difference between predicted and observed value (Rawat et al. 2013; Rawat et al. 2016; Rawat et al. 2017; Rawat et al. 2019b-e). The effect of each error on RMSE is proportional to total squared error and represented by eqn. (2):

$$\text{RMSE} = \sqrt{(n^{-1}\sum_{i=1}^{n}(V_M - V_O)^2)} \quad (2)$$

2.3.3 *Relative RMSE (R-RMSE)*

R-RMSE is to assess regression model results in predicting value (Rawat et al. 2013). It indicates the absolute fit of the model to the data points are the models predicted value. The best model fit depends on the objective and expressed by eqn. (3).

$$\text{R-RMSE} = \sqrt{n^{-1}}\sum_{i=1}^{n}\left(\frac{V_M - V_O}{V_M}\right)^2 \quad (3)$$

2.3.4 Percentage RMSE (% RMSE)

It is expressed as percentage of the datasets or models with different scales (Rawat et al. 2013). It would depend on the size of the range of the measured data. Percentage RMSE is highly useful in the unexpected values like very high or very low value and formulated as eqn. (4):

$$\%\ \text{RMSE} = \left(\frac{RMSE}{\sum_{i=1}^{n} V_O} \times 100\right) \quad (4)$$

ISSN- 2394-5125VOL 7, ISSUE 15, 2020

2.3.5 ***Volume Error (VE)***

Volume Error explains the error occurs while computing the volume of any surface with respect to x, y and z axis in which z is the altitude in 3 dimension of the plain E is the volume error of one cell to check the volume error in every cell of the volume. A piece cell of volume base has length and breadth and expressed as eqn. (5):

$$\boldsymbol{VE = n^{-1} \sum_{i=1}^{n} \left| \frac{V_O - V_M}{V_M} \right|} \quad (5)$$

2.3.6 ***Correlation Coefficient (CORR)***

Pearson correlation coefficient is bivariate correlation and value range from +1 to −1 (Rawat et al. 2013; Rawat et al. 2020 a & b). The +1 (positive correlation), 0 (no linear correlation), and −1 (total negative linear correlation) and expressed by eqn. (6):

$$\boldsymbol{CORR}\% = \frac{\boldsymbol{Cov(V_M.V_O)}}{\boldsymbol{\sigma V_M \, X \, \sigma V_O}} \quad (6)$$

2.3.7 ***Normalized RMSE***

The normalised RMSE (NRMSE) relate RMSE to the determined range of the variable. N-RMSE expressed as the percentage where low value indicate less residual variance. It can be calculated using eqn. (7):

$$\text{N-RMSE} = \frac{\sqrt{n \sum_{i=1}^{n} (V_M - V_O)^2}}{V_O} \quad (7)$$

2.3.8 ***Mean Absolute Error (MAE)***

Mean absolute error (MAE) is a measure of difference between two continuous variables. MAE use same scale as data being measured and scale dependent accuracy. This method is easier than RMSE and formula is given below (8):

$$\text{MAE} = \frac{\sum_{i=1}^{n} |V_O - V_M|}{n} \quad (8)$$

2.3.9 ***Mean Bias Error (MBE)***

Mean Bias Error (MBE) is the difference between observed and mean observation in a model. It is calculated as the sample variation and sample standard deviation the biasing can be done based on median and difference between variance of medium and estimate of the outcome divided by number of numbers of value and expressed as eqn. (9).

$$\boldsymbol{MBE = \frac{\sum_{n=1}^{n} (V_M - EV_O)}{n}} \quad (9)$$

2.3.10 ***Mean Absolute Percentage Error***

Mean Absolute Percentage Error (MAPE) is defined as parentage measure of predict versus estimated value. This formula is used to check accuracy of the any values in which it is equal to the percentage of submission of the actual upon theoretical value upon the total number of value and expressed as eqn. (10):

$$\boldsymbol{MAPE = \frac{\sum_{i=1}^{n} \left| \frac{V_O - V_M}{V_O} X100 \right|}{n}} \quad (10)$$

2.3.11 ***Index of Agreement (d)***

It helps to calculate the prediction of error model the values vary from zero to one and helps in predicting degree of order as it basically the ratio between potential and mean square error and presented as eqn. (11):

$$\boldsymbol{d = 1 - \frac{\sum_{i=1}^{n} (V_M - V_O)^2}{\sum_{i=1}^{n} (|V_M - \overline{V_O}| + |V_O + \overline{V_O}|)^2}} \quad (11)$$

2.3.12 ***Average Index Ratio (IR)***

It is a ratio of model versus observed value. If ratio is lower than one means the measured value is higher compared to observed value and expressed as eqn. (12):

ISSN- 2394-5125VOL 7, ISSUE 15, 2020

$$IR = \frac{V_M}{V_O} \quad (12)$$

2.3.13 ***Percentage of Error (PE)***

Percentage of error (PE) which explains the ratio between measured value minus observed value upon observed value multiplied by hundred and calculated as eqn. (13):

$$PE = \left(\frac{V_M - V_O}{V_O}\right) X100 \quad (13)$$

2.4 Ranking of Empirical Mathematical Models

Factor K was estimated to provide proper weight to select statistical index (all used statistical test) as follows eqn. (14-15):

$$K = \left[1 \Big/ \sum_{n=1}^{n} \left(1 \Big/ i_n \right) \right] \quad (14)$$

$$W_n = \frac{K}{i_n} \text{ and } 1 = \sum_1^n W_n \; Rating = \sum_{n=1}^{n} (W_n . i_n) \quad (15)$$

where, *K* is factor, *i* is n^{th} statistical index and *W* is weight for statistical index. Lowest ratting model will be on first rank and vice versa.

III. RESULT AND DISCUSSION

The overall statistics of elevation is maximum, minimum, mean and standard deviation of elevation values are obtained to examine differences in elevation in different DEM. Results are presented in Table 2. Table 2, there is a little change in the computed statistics for elevation where the percentage change around 0.54 % between the highest (from SRTM 90m and ASTER 30m) and lowest (from GE) value for the maximum elevation where maximum elevation values exhibited 2770m computed from the SRTM 90m and ASTER 30m DEM, and 2768m computed from the 30m SRTM DEM. This indicates that with the digital elevation models that have smallest cell size the maximum elevation becomes slightly underestimated.

Table 2 Summary statistics for elevation

Elevation data from	Summary statistics for elevation			
	Max (m)	Min (m)	Mean (m)	Std dev.
SRTM	2768	334	1485	506.79
SRTM	2770	334	1486	506.57
ASTER	2770	334	1485	506.50
Google earth	2716	332	1475	503.90

3.1 Statistical tests

3.1 Statistical tests for Settlement class at different height of ranges

Fig. 2 show a correlation between elevation of (i) toposheet vs. SRTM-30m, (ii) toposheet vs. SRTM-90m, (iii) toposheet vs. ASTER-30m, (iv) toposheet vs. GE at height range of 500 to 1100m and it show a very good result. In each condition correlation is higher because data sets from toposheet and different models are very close. Hence, it was not a correct logic to assign rating and rank only on basis of correlation, therefore we used 12 statistical test (SEE_M, RMSE, R-RMSE, %RMSE, VE, NRMSE, MAE, MBE, MAPE, *d*, IR and PE) rather than correlation (CORR) test. Fig. 2, demonstrated all three (ASTER-30m, SRTM-90m and ASTER-30m) models which are showing a good response with respect to elevation (at H1 range) from SOI toposheet. Although this performance is based on only correlation statistical test rather than all 12 statistical tests. Based on Table 3 and 4, ASTER-30m show a better result in comparison of other models therefore, ASTER-30m was ranked as first.

From Fig. 3, 2D scatter plot of elevation at H2 range of settlement over the area of interest. Settlement height under different elevation category can be measured using SAR technology because microwave signal can reach to the settlement and give the correct information of settlement height with high resolution of sensing like in case of

ISSN- 2394-5125VOL 7, ISSUE 15, 2020

SRTM-30m. Correct information of settlement height using SAR technology is effective, if settlement is not very dense. If settlement is dense, so many refractions will be generated due to corner effect of building. But in case of hill region settlement are not dense most of time. In case of thermal sensor, we can also collect correct elevation information for settlement, if distance between two buildings is enough (in hilly region), thermal emission will be clear from each building. Both the SRTM (30 m & 90m) and ASTER-30m show a good correlation with SOI toposheet. From Table 5 at H2 range, SRTM-90m DEM model show a good statistical result for settlement category. While Table 6 show SRTM-90m DEM model ranked as first.

From Fig. 4, graphical representation of elevation (from different models and real/reference elevation value from SOI toposheet) at H3 (1500—2400m) range of settlement over the study area. Settlement elevation under highest or top of hill elevation range category of settlement can be measured clearly using SRTM, but its resolution must be high (like 30 meter). Based on R^2 test SRTM-30m, SRTM-90m, ASTER-30m and GE model show good correlation value of 1.0, 1.0, 0.99, and 0.998 with reference elevation values. Table 7 and 8 reveal that at elevation range of H3, settlement height (at H3 range) can simulate with SRTM-30m model because SRTM-30m model ranked as first. In present study we not only analysed class data set, whereas we also attended different class with different range of height r1, H2, and H3, because in SAR analysis at different range of hill height is always matter.

From Fig. 5, a correlation between forest at H1 range of 600—1200m from different models (SRTM-30m, SRTM-90m, ASTER-30m and GE elevation) and SOI topographic sheet. From Table 9 and 10, at range of 600—1200m elevation, predicted elevation for forest from SRTM-30m model is good with rank of one. It indicates that SRTM-30m has more potential to predict elevation near to original elevation from SOI topographic sheet.

Fig. 6, is representation of graphical correlation between forest at elevation range of 1100—1800m (H2) from models and reference elevation of forest from SOI toposheet. SRTM-30m and SRTM-90m model are better than other two model. Table 11 and 12, model SRTM-90m and SRTM-30m ranked as first and second, respectively. It may be due to image resolution (90 m) which is affective at height range of H2. But such type of evidence is not revealed by statistical analysis.

Fig. 7 is statistical representation of model performance with respect to SOI toposheet, elevation at range of 2000—2600m (H3). The correlation value for model with respect to SOI toposheet are 1.00, 1.00, 0.99 and 0.97 for SRTM (30m & 90m), ASTER-30m and GE, respectively. The correlation the SRTM (30m & 90m) has showed a good performance with high range of hill (H3). From Table 13 and 14 are tabulated forms of statistical performance of models with respect to SOI topographic sheet elevation at range of 2000—2600m (H3). Based on Table 13 and 14, rank of models is followed as SRTM-30m (first), SRTM-90m (second), ASTER-30m (third) and Google Earth (fourth).

ISSN- 2394-5125VOL 7, ISSUE 15, 2020

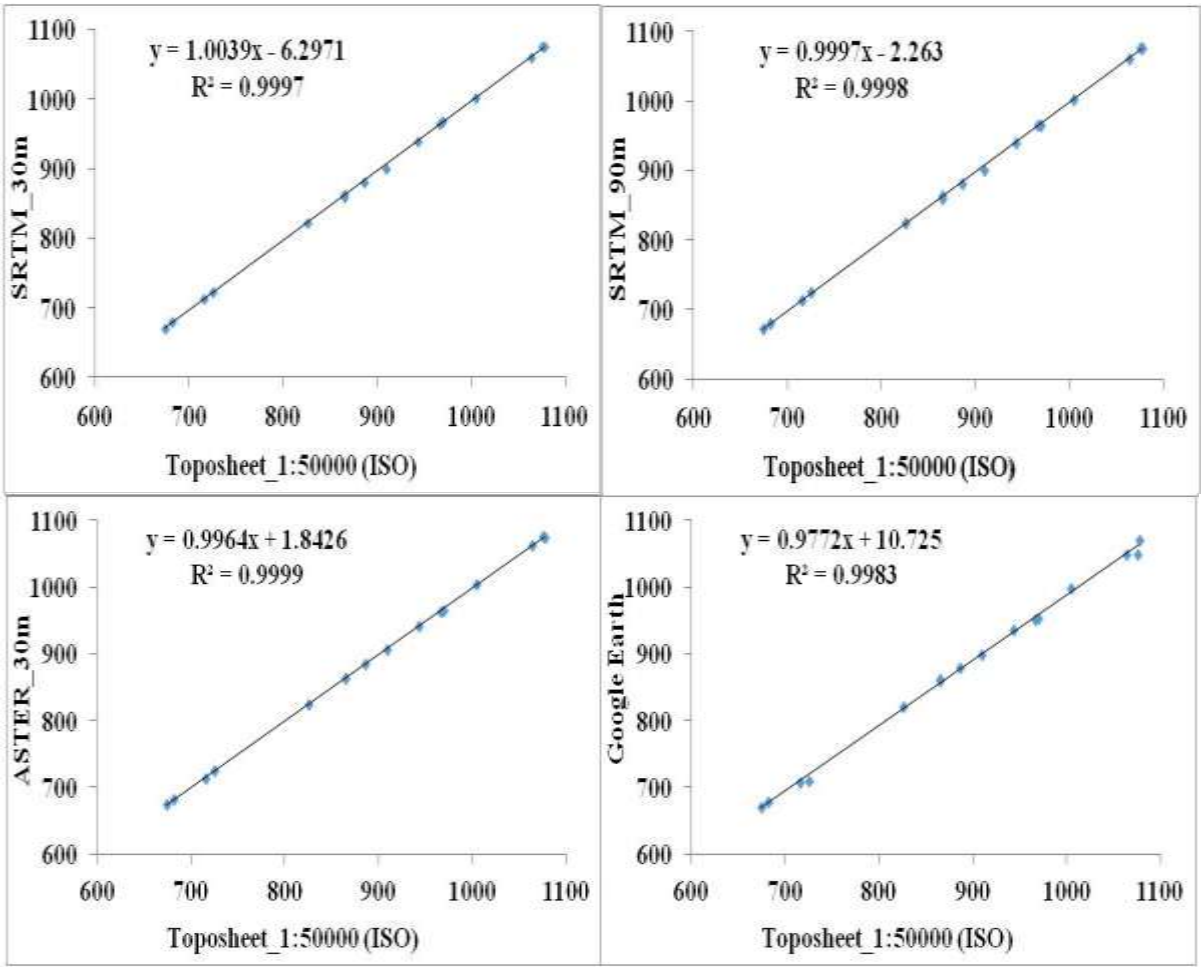

Fig. 2 Data sets of settlement class at range of height 600—1100m (H1)

ISSN- 2394-5125VOL 7, ISSUE 15, 2020

Table 3 Statistical tests result for settlement class at H1 range

Model	Statistical tests													K
	1	2	3	4	5	6	7	8	9	10	11	12	13	
SRTM_30	3.71	3.60	0.00	0.53	0.00	1.00	0.00	2.81	-2.81	0.33	1.00	1.00	-5.30	0.0013
SRTM_90	3.34	3.23	0.00	0.48	0.00	1.00	0.00	2.56	-2.56	0.29	1.00	1.00	-4.68	0.0011
ASTER_30	2.10	2.03	0.00	0.30	0.00	1.00	0.00	1.38	-1.38	0.15	1.00	1.00	-2.39	0.0006
Google Earth Elevation	11.73	11.36	0.01	1.68	0.01	1.00	0.01	9.56	-9.56	1.06	1.00	0.99	-16.78	0.0039

Table 4 Ranking and performance evaluation of each model for settlement class at H1 range

Assigning of Weightage to each statistical test													Rating	Rank	DEMs Model
1W	2 W	3 W	4W	5 W	6W	7 W	8W	9W	10 W	11 W	12 W	13W			
0.0003	0.0004	0.30	0.02	0.38	0.01	0.31	0.0004	-0.0004	0.0038	0.0013	0.0013	-0.0002	0.016	3	SRTM_30
0.0003	0.0003	0.30	0.02	0.38	0.01	0.31	0.0004	-0.0004	0.0038	0.0011	0.0011	-0.0002	0.014	2	SRTM_90
0.0003	0.0003	0.29	0.02	0.42	0.01	0.28	0.0005	-0.0005	0.0042	0.0006	0.0006	-0.0003	0.008	1	ASTER_30
0.0003	0.0003	0.31	0.02	0.36	0.04	0.30	0.0004	-0.0004	0.0036	0.0039	0.0039	-0.0002	0.050	4	Google Earth Elevation

ISSN- 2394-5125VOL 7, ISSUE 15, 2020

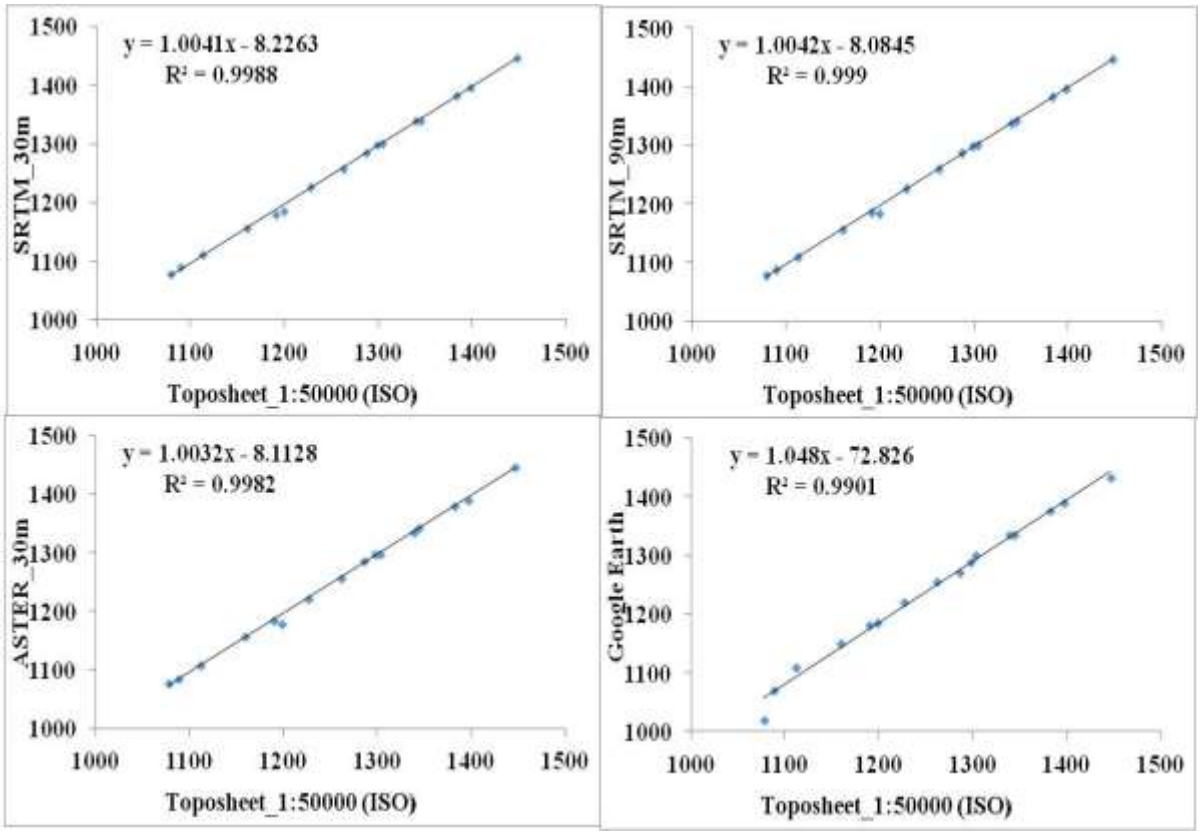

Fig. 3 Data sets of settlement class at height range of 1100—1500m (H2)

ISSN- 2394-5125VOL 7, ISSUE 15, 2020

Table 5 Statistical tests result for settlement class at H2 range

	Statistical test													
Model	**1**	**2**	**3**	**4**	**5**	**6**	**7**	**8**	**9**	**10**	**11**	**12**	**13**	**K**
SRTM_30	5.073	4.912	0.004	0.456	0.003	0.999	0.004	3.13	-3.13	0.25	1.00	1.00	-4.04	0.0011
SRTM_90	4.590	4.444	0.004	0.412	0.002	1.000	0.004	2.75	-2.75	0.22	1.00	1.00	-3.57	0.0010
ASTER_30	6.434	6.230	0.005	0.578	0.003	0.999	0.005	4.06	-4.06	0.33	1.00	1.00	-5.23	0.0014
Google Earth Elevation	18.334	17.752	0.016	1.647	0.011	0.995	0.014	12.50	-12.50	1.07	0.99	0.99	-16.68	0.0044

Table 6 Ranking and performance evaluation of each model for settlement class at H2 range

Assigning of Weightage to each statistical test													Rating	Rank	DEMs Model
1W	**2W**	**3W**	**4W**	**5W**	**6W**	**7W**	**8W**	**9W**	**10W**	**11W**	**12W**	**13W**			
0.0002	0.0002	0.27	0.00	0.44	0.001	0.28	0.0004	-0.0004	0.004	0.001	0.001	-0.0003	0.014	2	SRTM_30
0.0002	0.0002	0.27	0.00	0.44	0.001	0.28	0.0004	-0.0004	0.004	0.001	0.001	-0.0003	0.013	1	SRTM_90
0.0002	0.0002	0.27	0.00	0.43	0.001	0.29	0.0003	-0.0003	0.004	0.001	0.001	-0.0003	0.018	3	ASTER_30
0.0002	0.0002	0.26	0.00	0.41	0.004	0.31	0.0003	-0.0003	0.004	0.004	0.004	-0.0003	0.057	4	Google Earth Elevation

ISSN- 2394-5125VOL 7, ISSUE 15, 2020

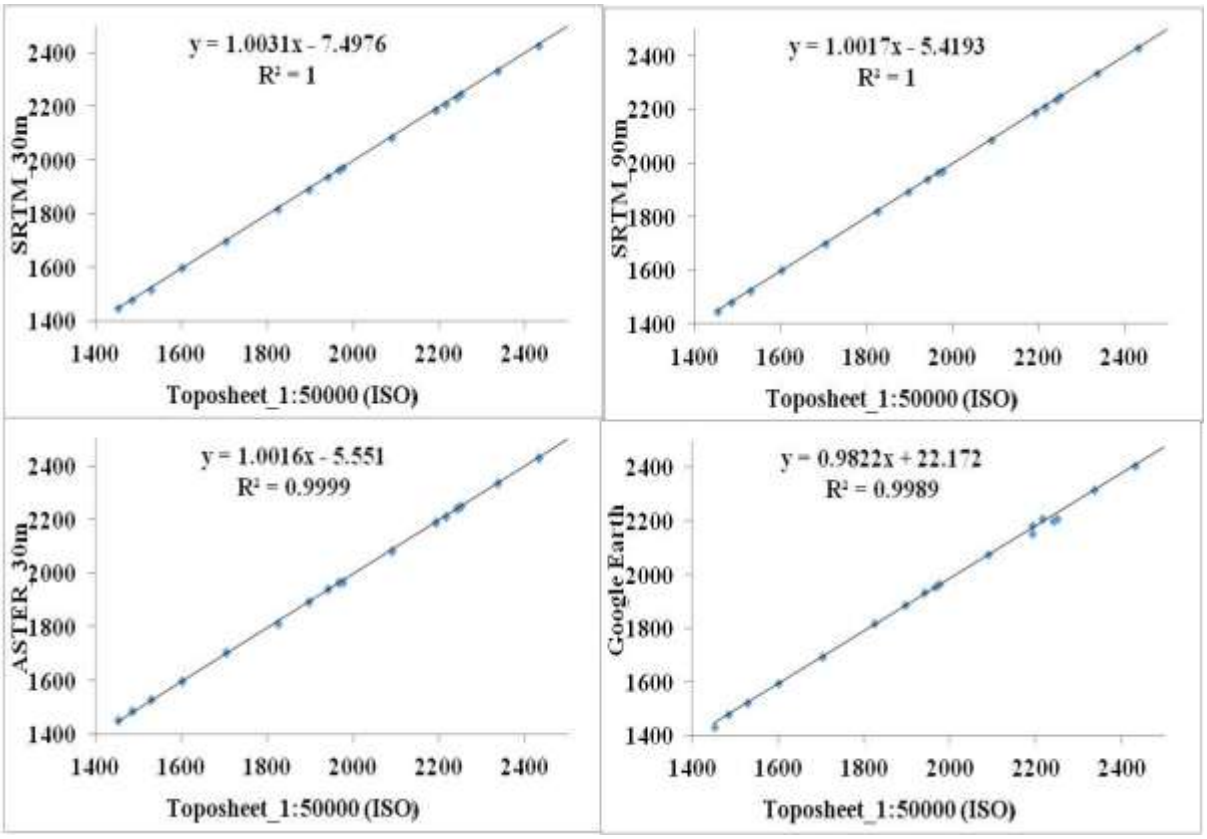

Fig. 4 Data sets of settlement class at height of 1500—2400m (H3)

ISSN- 2394-5125VOL 7, ISSUE 15, 2020

Table 7 Statistical tests result for settlement class at height of H3

Model	Statistical test													K
	1	2	3	4	5	6	7	8	9	10	11	12	13	
SRTM_30	2.6	2.6	0.002	0.18	0.001	1.0	0.001	1.4	-1.4	0.09	1.0	0.999	-1.5	0.00039
SRTM_90	2.7	2.6	0.001	0.18	0.001	1.0	0.001	2.1	-2.1	0.11	1.0	0.999	-2.1	0.00042
ASTER_30	4.5	4.4	0.002	0.30	0.001	1.0	0.002	2.4	-2.4	0.13	1.0	0.999	-2.4	0.00059
Google Earth Elevation	18.4	17.9	0.008	1.23	0.006	0.9	0.009	13.3	-13.3	0.65	0.9	0.993	-12.1	0.00256

Table 8 Ranking and performance evaluation of each model for settlement class at H3

Assigning of Weightage to each statistical test												Rating	Rank	DEMs Model
1W	2W	3W	4W	5W	6W	7W	8W	9W	10W	11W	12W	13W			
0.0001	0.0002	0.25	0.02	0.44	0.0004	0.30	0.003	-0.0003	0.004	0.0004	0.0004	-0.0003	0.005	1	SRTM_30
0.0002	0.0002	0.29	0.02	0.37	0.0004	0.33	0.002	-0.0002	0.004	0.0004	0.0004	-0.0002	0.006	2	SRTM_90
0.0001	0.0001	0.26	0.02	0.46	0.0006	0.27	0.002	-0.0002	0.005	0.0006	0.0006	-0.0002	0.008	3	ASTER_30
0.0001	0.0001	0.30	0.02	0.40	0.0026	0.28	0.002	-0.0002	0.004	0.0026	0.0026	-0.0002	0.033	4	Google Earth Elevation

ISSN- 2394-5125VOL 7, ISSUE 15, 2020

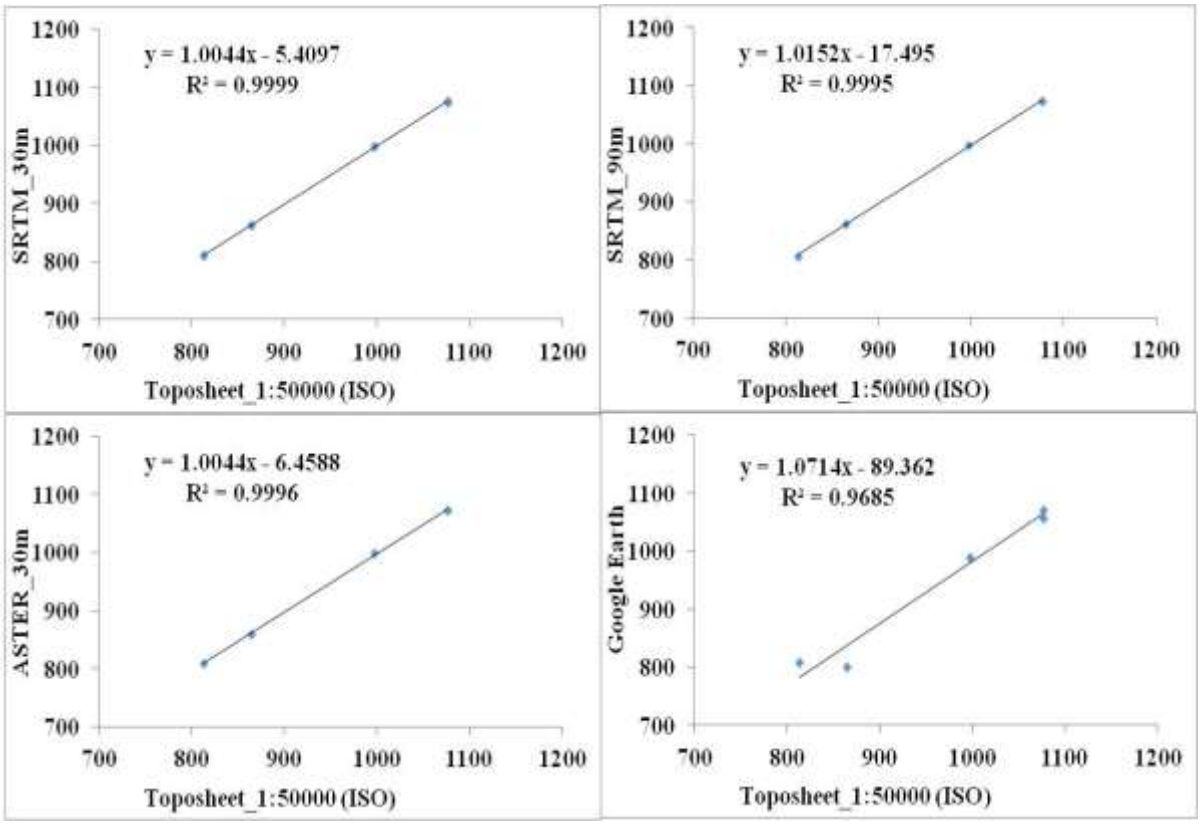

Fig. 5 Data sets of forest class at height of 600—1200m (H1)

ISSN- 2394-5125VOL 7, ISSUE 15, 2020

Table 9 Statistical tests result for forest class at height range of H1

Model	Statistical test													K
	1	2	3	4	5	6	7	8	9	10	11	12	13	
SRTM_30	2.00	1.79	0.00	0.22	0.00	1.00	0.00	1.2	-1.2	0.2	1.0	1.0	-0.7	0.0006
SRTM_90	4.53	4.05	0.00	0.50	0.00	1.00	0.00	2.8	-2.8	0.4	1.0	1.0	-1.6	0.0014
ASTER_30	3.43	3.07	0.00	0.38	0.00	1.00	0.00	2.2	-2.2	0.3	1.0	1.0	-1.2	0.0011
Google Earth Elevation	33.85	30.27	0.04	3.72	0.02	0.98	0.03	20.4	-20.4	2.4	1.0	1.0	-11.1	0.0095

Table 10 Ranking and performance evaluation of each model for Forest class at H1range

Assigning of Weightage to each statistical test													Rating	Rank	DEMs Model
1W	2W	3W	4W	5W	6W	7W	8W	9W	10W	11W	12W	13W			
0.00	0.00	0.30	0.00	0.36	0.00	0.33	0.00	0.00	0.00	0.00	0.00	0.00	0.008	1	SRTM_30
0.00	0.00	0.28	0.00	0.38	0.00	0.33	0.00	0.00	0.00	0.00	0.00	0.00	0.018	3	SRTM_90
0.00	0.00	0.32	0.00	0.33	0.00	0.34	0.00	0.00	0.00	0.00	0.00	0.00	0.014	2	ASTER_30
0.00	0.00	0.26	0.00	0.40	0.01	0.30	0.00	0.00	0.00	0.01	0.01	0.00	0.124	4	Google Earth Elevation

ISSN- 2394-5125VOL 7, ISSUE 15, 2020

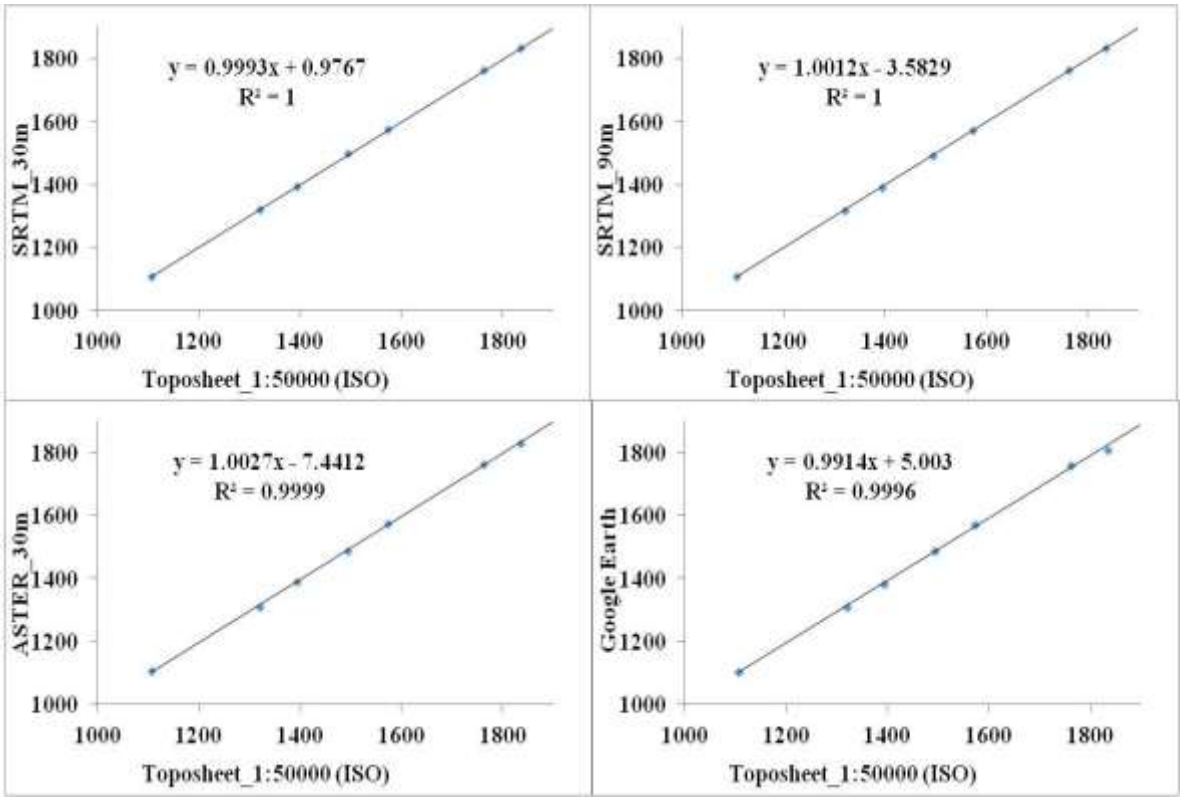

Fig. 6 Data sets of forest class at elevation range of 1100—1800m (H2)

ISSN- 2394-5125VOL 7, ISSUE 15, 2020

Table 11 Statistical tests result for forest class at range of 1100—1800m (H2)

Model	Statistical test													K
	1	2	3	4	5	6	7	8	9	10	11	12	13	
SRTM_30	1.78	1.71	0.00	0.15	0.00	1.00	0.00	0.25	-0.25	0.07	1.00	1.00	-0.16	0.0005
SRTM_90	2.09	2.00	0.00	0.18	0.00	1.00	0.00	1.50	-1.50	0.10	1.00	1.00	-1.14	0.0004
ASTER_30	4.38	4.19	0.18	0.38	0.00	1.00	0.00	2.92	-2.92	0.19	1.00	1.00	-2.24	0.0012
Google Earth Elevation	11.67	11.17	0.01	1.01	0.01	1.00	0.01	9.42	-9.42	0.56	1.00	0.99	-6.62	0.0022

Table 12 Ranking and performance evaluation of each model for forest class at range of 1100—1800m (H2)

Assigning of Weightage to each statistical test													Rating	Rank	DEMs Model
1W	2W	3W	4W	5W	6W	7W	8W	9W	10W	11W	12W	13W			
0.00	0.00	0.26	0.00	0.28	0.00	0.45	0.00	0.00	0.01	0.00	0.00	0.00	0.006	2	SRTM_30
0.00	0.00	0.22	0.00	0.39	0.00	0.38	0.00	0.00	0.00	0.00	0.00	0.00	0.005	1	SRTM_90
0.00	0.00	0.01	0.00	0.52	0.00	0.46	0.00	0.00	0.01	0.00	0.00	0.00	0.015	3	ASTER_30
0.00	0.00	0.34	0.00	0.33	0.00	0.33	0.00	0.00	0.00	0.00	0.00	0.00	0.028	4	Google Earth Elevation

ISSN- 2394-5125VOL 7, ISSUE 15, 2020

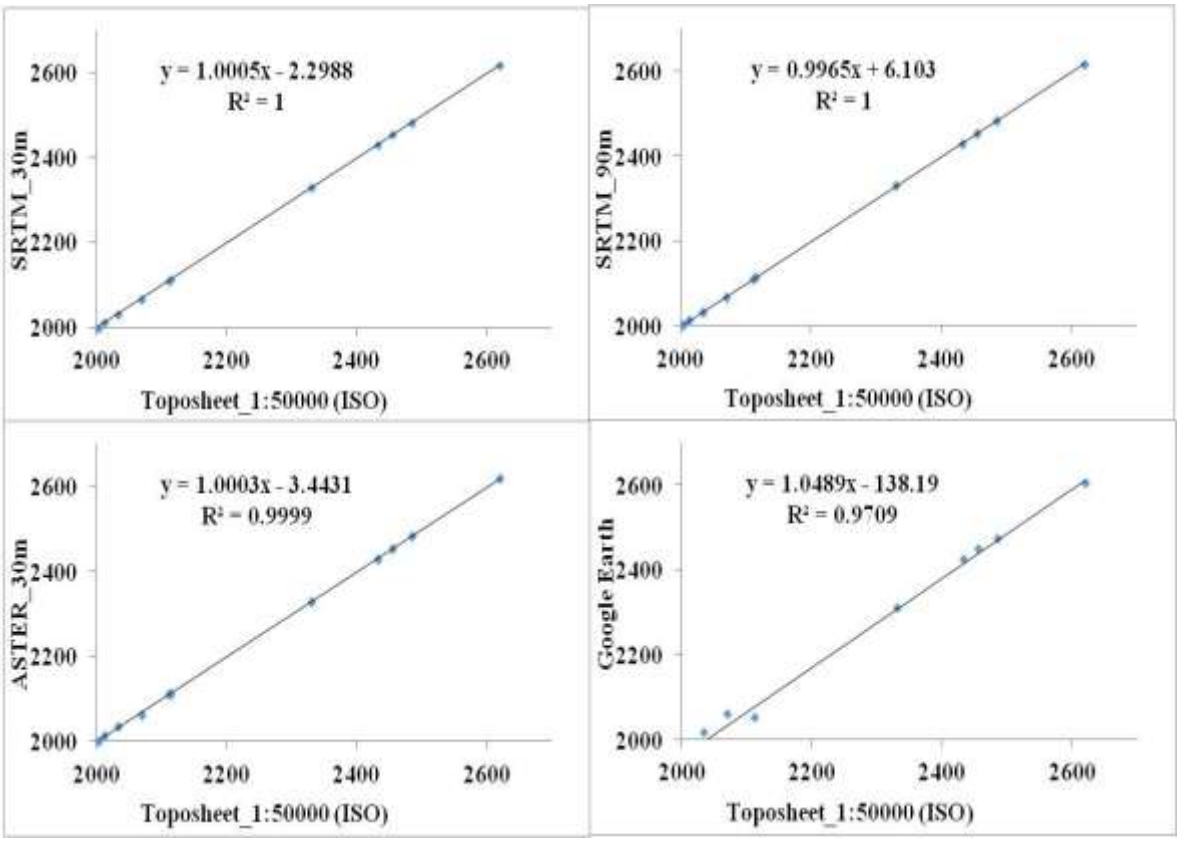

Fig. 7 Data sets of forest class at height range of 2000—2600m (H3)

ISSN- 2394-5125VOL 7, ISSUE 15, 2020

Table 13 Statistical tests result for forest class at range of 2000—2600m (H3)

Model	Statistical test													K
	1	2	3	4	5	6	7	8	9	10	11	12	13	
SRTM_30	1.55	1.48	0.00	0.07	0.00	1.00	0.00	1.27	-1.27	0.06	1.00	1.00	-0.63	0.0002
SRTM_90	2.32	2.22	0.00	0.11	0.00	1.00	0.00	1.82	-1.82	0.08	1.00	1.00	-0.87	0.0003
ASTER_30	3.58	3.41	0.00	0.17	0.00	1.00	0.00	2.73	-2.73	0.12	1.00	1.00	-1.35	0.0005
Google Earth Elevation	51.80	49.39	0.02	2.47	0.02	0.99	0.02	28.45	-28.45	1.38	1.00	0.99	-14.53	0.0064

Table 14 Ranking and performance evaluation of each model for forest class at rage of 2000—2600m (H3)

Assigning of Weightage to each statistical test													Rating	Rank	DEMs Model
1W	2W	3W	4W	5W	6W	7W	8W	9W	10W	11W	12W	13W			
0.0001	0.0001	0.32	0.0030	0.34	0.0002	0.33	0.0002	-0.002	0.0038	0.0002	0.0002	-0.003	0.0033	1	SRTM_30
0.0001	0.0001	0.33	0.0028	0.35	0.0003	0.31	0.0002	-0.002	0.0039	0.0003	0.0003	-0.004	0.0034	2	SRTM_90
0.0001	0.0001	0.31	0.0029	0.36	0.0005	0.32	0.0002	-0.002	0.0040	0.0005	0.0005	-0.004	0.0036	3	ASTER_30
0.0001	0.0001	0.26	0.0026	0.42	0.0065	0.29	0.0002	-0.002	0.0047	0.0064	0.0065	-0.004	0.0833	4	Google Earth Elevation

ISSN- 2394-5125VOL 7, ISSUE 15, 2020

IV. CONCLUSION

This research evaluates the vertical accuracy of DEM data using the statistical performance measures. In open land with flat terrain, the extracted elevation from SRTM-30m achieved high accuracy. The results of this study illustrate higher accuracy for SRTM-30m and ASTER-30m, which was coherent with the spatial resolution of the input dataset. In most cases, a high-resolution DEM based elevation information improved vertical accuracy; however, there were several noisy effects in these DEMs, specifically at the borders and corners of man-made structures, which require further, processing of high-resolution DEM. Although the SRTM-30m DEM had 30m grid spacing, it could be deduced that this was due to the acquisition of strong signals from the original less than 30m DEM, which was produced from the 10m SAR images. The accuracies of the DEMs varied with respect to different height range (H1, H2 and H3) and different categories/classes.

The maximum RMSE of 38.29m was recorded for forest class by GE model with respect to reference data sets. While minimum RMSE of 1.57m was recorded for temples by SRTM-30m model with respect to SOI toposheet based data. RMSEs range between 1.57m (minimum for temple classes) to 3.75m (maximum for settlement classes) and SEE_M 1.61(minimum for temple classes) to 3.79m (maximum for settlement classes) for SRTM-30m while ASTER-30m show minimum RMSE 1.84m (minimum for temple class) and maximum 4.54m (for settlement class) respectively. SRTM-30m DEMs produced better elevation accuracy value for rare settlement classes when the elevation differences were not considerable. While comparing the different DEMs, the source of the data became more important, especially for hilly regions.

ACKNOWLEDGMENT

This research work is part of M. Tech. thesis (of Mr. Sidhartha Sawai) and authors wish to express their thanks to the HOD and Vice Chancellor of the University for providing the necessary arrangements. We are grateful to the Editor in Chief of the journal and reviewers.

REFERENCES

[1] Arun, P. V. (2013). A comparative analysis of different DEM interpolation methods. The Egyptian Journal of Remote Sensing and Space Science, 16(2), 133-139.
[2] Choudhari, P. P., Nigam, G. K., Singh, S. K., & Thakur, S. (2018). Morphometric based prioritization of watershed for groundwater potential of Mula river basin, Maharashtra, India. Geology, Ecology, and Landscapes, 2(4), 256-267.
[3] Das, S., Patel, P. P., & Sengupta, S. (2016). Evaluation of different digital elevation models for analyzing drainage morphometric parameters in a mountainous terrain: a case study of the Supin–Upper Tons Basin, Indian Himalayas. SpringerPlus, 5(1), 1544.
[4] Kumar Pradhan, R., Srivastava, P. K., Maurya, S., Kumar Singh, S., & Patel, D. P. (2020). Integrated framework for soil and water conservation in Kosi River Basin. Geocarto International, 35(4), 391-410.
[5] Kumar, N., Singh, S. K., Singh, V. G., & Dzwairo, B. (2018a). Investigation of impacts of land use/land cover change on water availability of Tons River Basin, Madhya Pradesh, India. Modeling Earth Systems and Environment, 4(1), 295-310.
[6] Kumar, N., Singh, S. K., & Pandey, H. K. (2018b). Drainage morphometric analysis using open access earth observation datasets in a drought-affected part of Bundelkhand, India. Applied Geomatics, 10(3), 173-189.
[7] Kumar, N., Singh, S. K., Srivastava, P. K., & Narsimlu, B. (2017). SWAT Model calibration and uncertainty analysis for streamflow prediction of the Tons River Basin, India, using Sequential Uncertainty Fitting (SUFI-2) algorithm. Modeling Earth Systems and Environment, 3(1), 30.
[8] Li, H., & Zhao, J. (2018). Evaluation of the newly released worldwide AW3D30 DEM over typical landforms of China using two global DEMs and ICESat/GLAS data. IEEE Journal of Selected Topics in Applied Earth Observations and Remote Sensing, 11(11), 4430-4440.
[9] Maliqi, E., & Singh, S. K. (2019). Quantitative Estimation of Soil Erosion Using Open-Access Earth Observation Data Sets and Erosion Potential Model. Water Conservation Science and Engineering, 4(4), 187-200.
[10] Murmu, P., Kumar, M., Lal, D., Sonker, I., & Singh, S. K. (2019). Delineation of groundwater potential zones using geospatial techniques and analytical hierarchy process in Dumka district, Jharkhand, India. Groundwater for Sustainable Development, 9, 100239.
[11] Narsimlu, B., Gosain, A. K., Chahar, B. R., Singh, S. K., & Srivastava, P. K. (2015). SWAT model calibration and uncertainty analysis for streamflow prediction in the Kunwari River Basin, India, using sequential uncertainty fitting. Environmental Processes, 2(1), 79-95.

[12] Pande, C. B., Moharir, K. N., Singh, S. K., & Varade, A. M. (2019). An integrated approach to delineate the groundwater potential zones in Devdari watershed area of Akola district, Maharashtra, Central India. Environment, Development and Sustainability, 1-21.
[13] Patel, A., Katiyar, S. K., & Prasad, V. (2016). Performances evaluation of different open source DEM using Differential Global Positioning System (DGPS). The Egyptian Journal of Remote Sensing and Space Science, 19(1), 7-16.
[14] Rawat, K.S, Singh, S.K. & Ray, R.L., Szabo, S., & Kumar, S. (2020a). Parameterizing the modified water cloud model to improve soil moisture data retrieval using vegetation models. Hungarian Geographical Bulletin, 69(1), 17-26. DOI: 10.15201/hungeo bull. 69.1. 2
[15] Rawat, K.S., Singh, S.K., Ray, R.L., & Szabo, S. (2020b). Parameterization of Modified Water Cloud Model (MWCM) using Normalized Difference Vegetation Index (NDVI) for winter wheat crop: a case study. Geocarto International, DOI: 10.1080/10106049.2020.1783579
[16] Rawat, K.S., Singh, S.K., Singh, M.I., & Garg, B.L. (2019a). Comparative evaluation of vertical accuracy of elevated points with ground control points from ASTERDEM and SRTMDEM with respect to CARTOSAT-1DEM. Remote Sensing Applications: Society and Environment, 13, 289-297.
[17] Rawat, K.S., Pradhan S., Tripathi, V.K., Lordwin, J., & Singh, S. K. (2019b). Statistical approach to evaluate groundwater contamination for drinking and irrigation suitability. Groundwater for Sustainable Development, 9, 1-12, https://doi.org/10.1016/j.gsd.2019.100251.
[18] Rawat, K.S., Singh, S.K., & Pal, R.K. (2019vc). Synergetic methodology for estimation of soil moisture over agricultural area Using Landsat-8 and Sentinel-1 satellite data. Remote sensing Application: Society and environment, 15(2019)100250. https://doi.org/10.1016/j.rsase.2019.100250
[19] Rawat, K.S., Singh, S.K., & Ray, R.L. (2019d). An integrated approach to estimate surface soil moisture in agricultural lands. Geocarto International, doi.org/10.1080/10106049.2019.1678674
[20] Rawat, KS, Singh, S.K. & Bala A, (2019e). Estimation of crop evapotranspiration through spatial distributed crop coefficient in a semi-arid environment. Agricultural Water Management, 213(1), 922-933
[21] Rawat, K.S., Bala, A., Singh, S.K., & Pal, R.K. (2017). Quantification of wheat crop evapotranspiration and mapping: a case study from Bhiwani District of Haryana, India. Agricultural Water Management, 187, 200-209.
[22] Rawat, K.S., & Mishra, A.K. (2016). Evaluation of Relief aspects Morphometric Parameters derived from different sources of DEMs and its effects over time of concentration of runoff (T_C). Earth Science Informatics, 9, 409-424.
[23] Rawat, K.S., Mishra, A.K., Sehgal, V.K. & Tripathi, V.K. (2013). Comparative evaluation of horizontal accuracy of elevations of selected ground control points from ASTER and SRTM DEM with respect to CARTOSAT-1 DEM: A case study of district Shahjahanpur (Uttar Pradesh), India. Geocarto International, 28(5), 439-452.
[24] Rusli, N., Majid, M. R., & Din, A. H. M. (2014, February). Google Earth's derived digital elevation model: A comparative assessment with Aster and SRTM data. In IOP Conference Series: Earth and Environmental Science (Vol. 18, No. 1, p. 012065). IOP Publishing.
[25] Singh, S. K., Mustak, S., Srivastava, P. K., Szabó, S., & Islam, T. (2015). Predicting spatial and decadal LULC changes through cellular automata Markov chain models using earth observation datasets and geo-information. Environmental Processes, 2(1), 61-78.
[26] Singh, S., Singh, C., & Mukherjee, S. (2010). Impact of land-use and land-cover change on groundwater quality in the Lower Shiwalik hills: a remote sensing and GIS based approach. Open Geosciences, 2(2), 124-131.
[27] Singh, V., & Singh, S. K. (2018). Hypsometric Analysis Using Microwave Satellite Data and GIS of Naina–Gorma River Basin (Rewa district, Madhya Pradesh, India). Water Conservation Science and Engineering, 3(4), 221-234.
[28] Srivastava, P. K., Petropoulos, G. P., Gupta, M., Singh, S. K., Islam, T., & Loka, D. (2019). Deriving forest fire probability maps from the fusion of visible/infrared satellite data and geospatial data mining. Modeling Earth Systems and Environment, 5(2), 627-643.
[29] Stankevich, S., Piestova, I., Kozlova, A., Titarenko, O., & Singh, S. K. (2020). Satellite Radar Interferometry Processing and Elevation Change Analysis for Geoenvironmental Hazard Assessment. Techniques for Disaster Risk Management and Mitigation, 125-139.
[30] Suwandana, E., Kawamura, K., Sakuno, Y., Kustiyanto, E., &Raharjo, B. (2012). Evaluation of ASTER GDEM2 in comparison with GDEM1, SRTM DEM and topographic-map-derived DEM using inundation area analysis and RTK-dGPS data. Remote Sensing, 4(8), 2419-2431.
[31] Szabó, G., Singh, S. K., & Szabó, S. (2015). Slope angle and aspect as influencing factors on the accuracy of the SRTM and the ASTER GDEM databases. Physics and Chemistry of the Earth, Parts A/B/C, 83, 137-145.
[32] Yadav, S. K., Dubey, A., Singh, S. K., & Yadav, D. (2020). Spatial regionalisation of morphometric characteristics of mini watershed of Northern Foreland of Peninsular India. Arabian Journal of Geosciences, 13, 435.

ISSN- 2394-5125VOL 7, ISSUE 15, 2020

[33] Yadav, S. K., Dubey, A., Szilard, S., & Singh, S. K. (2018). Prioritisation of sub-watersheds based on earth observation data of agricultural dominated northern river basin of India. Geocarto International, 33(4), 339-356.
[34] Yadav, S. K., Singh, S. K., Gupta, M., & Srivastava, P. K. (2014). Morphometric analysis of Upper Tons basin from Northern Foreland of Peninsular India using CARTOSAT satellite and GIS. Geocarto International, 29(8), 895-914.
[35] Yarrakula, K., Deb, D., &Samanta, B. (2013). Comparative evaluation of Cartosat-1 and SRTM imageries for digital elevation modelling. Geo-spatial Information Science, 16(2), 75-82.